Journal of Bone and Mineral Metabolism (2019) 37:676–684
https://doi.org/10.1007/s00774-018-0975-3

ORIGINAL ARTICLE

Quantitation and distribution of metallic elements in sequestra of medication-related osteonecrosis of jaw (MRONJ) using inductively coupled plasma atomic emission spectroscopy and synchrotron radiation X-ray fluorescence analysis

Ruri Komiya[1] · Takahiro Wada[2] · Fumihiko Tsushima[1] · Kei Sakamoto[3] · Tohru Ikeda[3] · Akira Yamaguchi[3,4] · Hiroyuki Harada[1] · Motohiro Uo[2,5]

Received: 28 August 2018 / Accepted: 25 October 2018 / Published online: 22 November 2018

Abstract

Medication-related osteonecrosis of the jaw (MRONJ) is a serious adverse effect of antiresorptive agents like bisphosphonates. Abnormal concentrations of various trace metallic elements contained in bone minerals have been associated with MRONJ. In this study, we focused on trace metallic elements contained in the MRONJ sequestrum; their content and distribution were compared to those in osteomyelitis and non-inflammatory bones using inductively coupled plasma atomic emission spectroscopy (ICP-AES) and synchrotron radiation X-ray fluorescence analysis (SR-XRF). On ICP-AES analyses, various trace elements (Co, Cr, Cu, Fe, K, Mg, Ni, Sb, Ti, V, Pb) were significantly more in MRONJ sequestra than non-inflammatory bones. The Cu content was significantly higher in MRONJ sequestra than osteomyelitis and non-inflammatory bones. The Cu content in MRONJ sequestra was high even after decalcification. Additionally, Cu was distributed along the trabecular structures in decalcified MRONJ specimens, as observed using SR-XRF analysis. Therefore, this study was indicative of the characteristic behavior of Cu in MRONJ.

Keywords Medication-related osteonecrosis of the jaw (MRONJ) · Trace metallic element · Inductively coupled plasma atomic emission spectroscopy (ICP-AES) · Synchrotron radiation X-ray fluorescence analysis (SR-XRF)

Introduction

Medication-related osteonecrosis of the jaw (MRONJ) is a rare but serious adverse effect of antiresorptive or antiangiogenic agents that was first reported in 2003 in a patient who received bisphosphonate (BP) [1]. According to the American Association of Oral and Maxillofacial Surgeons, patients may be considered to have MRONJ if all of the following characteristics are present: (1) current or previous treatment with antiresorptive or antiangiogenic agents; (2) exposed bone or bone that can be probed through an intraoral or extra-oral fistula in the maxillofacial region and that has persisted for more than 8 weeks; and (3) no history of radiation therapy to the jaws or obvious metastatic disease to the jaws [2]. The risk of developing MRONJ was reported to be 0.7–8.5% among cancer patients treated with BP therapy [3, 4]. The risk of MRONJ for osteoporosis patients receiving BP therapy was reported to be 0.1% but increases to 0.21% among patients with more than 4 years of oral BP

Electronic supplementary material The online version of this article (https://doi.org/10.1007/s00774-018-0975-3) contains supplementary material, which is available to authorized users.

✉ Motohiro Uo
uo.abm@tmd.ac.jp

[1] Department of Oral and Maxillofacial Surgery, Graduate School of Medical and Dental Sciences, Tokyo Medical and Dental University, 1-5-45, Yushima, Bunkyo-ku, Tokyo, Japan

[2] Department of Advanced Biomaterials, Graduate School of Medical and Dental Sciences, Tokyo Medical and Dental University, 1-5-45, Yushima, Bunkyo-ku, Tokyo, Japan

[3] Department of Oral Pathology, Graduate School of Medical and Dental Sciences, Tokyo Medical and Dental University, 1-5-45, Yushima, Bunkyo-ku, Tokyo, Japan

[4] Oral Health Science Center, Tokyo Dental College, 2-9-18, Misakicho, Chiyoda-Ku, Tokyo 101-0061, Japan

[5] Department of Materials Engineering, Graduate School of Engineering, The University of Tokyo, 7-3-1, Hongo, Bunkyo-ku, Tokyo, Japan

exposure [5]. Recently, the risk for similar adverse effects was reported among patients receiving the receptor-activated nuclear factor kappa-B ligand (RANKL) inhibitor (denosumab), a different type of antiresorptive agent [6]. Importantly, invasive dental treatment—e.g., tooth extraction—triggers MRONJ in most cases [7]. However, the underlying mechanism of pathogenesis remains unclarified. To identify biomarkers associated with MRONJ, several studies have investigated changes in the chemical components of bones exhibiting MRONJ development [8, 9]; however, a clear association could not be found. On the other hand, various trace metallic elements contained in bone minerals offer an alternative avenue to study the pathogenesis of MRONJ. Cu and Zn are among the most typical factors assessed as potential markers by clinical laboratories. Concerning osteoporosis, disorder of plasma zinc (Zn) concentrations was reported among patients [10]. In addition, an association between BP treatment and decreases of Zn and Cu concentrations in the oral epithelium was reported by an animal experiment [11]. We aim to build upon such findings by focusing on the abnormal concentrations of trace metallic elements in patients with MRONJ sequestrum. A previous study that conducted a micro-scale elemental distribution analysis found an accumulation of Cu in the MRONJ sequestrum [12]. The present study performed a similar analysis using synchrotron radiation X-ray fluorescence (SR-XRF), a technique that emits extremely strong and highly collimated electromagnetic waves, including X-ray, and allows for high sensitivity in the analysis of micro-areas and the trace-element distribution of a specimen without inducing damage. However, accurate quantification of a trace element with SR-XRF is subject to limitations. The elemental distribution image that the method provides only indicates relative concentration. In addition, current SR-XRF facilities expose the optic to the air, which absorbs the fluorescent X-ray from light elements. The analysis of light elements (e.g., B, Al, Na), thus, becomes impossible. To reveal the effect of the trace elements in bone on MRONJ development, the quantitation of the trace metallic elements in MRONJ sequestra and a comparison of such data with other inflammatory or non-inflammatory disease bones were required to clarify the significance of the trace-element accumulation to the development of the condition. An alternative method was, therefore, required for the quantitative analysis of the trace elements in bones.

Inductively coupled plasma atomic emission spectroscopy (ICP-AES) is the most common method for highly sensitive trace-element detection (especially cation species) and accurate quantification in solution specimens. The technique is usually applied once the solid specimen is dissolved with acid treatment, which compromises the inhomogeneity of the trace elements and precludes the characterization of elemental distribution and localization by ICP-AES. Therefore, ICP-AES and SR-XRF are complementary methods for the analysis of trace elements inhomogeneously contained in solid specimens; the former obtains the distribution and localization of a trace element within a sequestra, while the latter allows for the trace element's quantitation.

Thus, the present investigation was aimed at quantifying and comparing the trace-metallic-element contents in MRONJ, osteomyelitis, and non-inflammatory bones using ICP-AES. The tested bones were then analyzed using SR-XRF to reveal elemental distributions. By the two different analytical methods in tandem, the relationship between MRONJ development and trace-metallic-element accumulation was further elucidated.

Materials and methods

Bone specimens

Bone specimens were supplied by Tokyo Medical and Dental University Hospital. The samples included 14 MRONJ-induced sequestrum specimens that had received antiresorptive agent (BP or denosumab) therapy, 10 osteomyelitis, and 6 torus mandibularis specimens that did not receive antiresorptive agent therapy. Osteomyelitis sequestrum is caused by infectious bone degradation not induced by an antiresorptive agent; these specimens were, therefore, used as a reference for inflammatory bone disease. The excised bones from jaw deformities and exostosis were used as an additional reference of non-inflammatory bone disease independent of exposure to medication and infection. All patients provided informed consent and the study protocol was approved by the Ethical Committee of Tokyo Medical and Dental University (D2016-002). Table 1 shows the clinical data for all specimens.

The present study conducted three analyses: (1) ICP-AES analysis without any sample treatment, e.g., fixation or decalcification; (2) SR-XRF elemental distribution; and (3) ICP-AES analysis with decalcification. The size of the specimens informed which analyses were applied: if the specimen was large enough, it was split into three parts and analyses 1–3 were performed (MR01, MR02, MR03, MR05, MR06, MR10); if the specimen was not large enough, it was halved and analyses 1–2 were conducted; the smaller specimens were used only for analysis 1. For analysis 3, half of the specimen was fixed in 4% phosphate-buffered saline–formalin, and decalcification was performed with Plank–Rychlo solution before the ICP-AES analysis to ascertain the effect of decalcification process for the trace-element concentration.

For analysis 2, the specimen was fixed and decalcified according to the aforementioned method, embedded in paraffin, and sliced into two thicknesses (4 μm and 10 μm). The

Table 1 List of specimens used in this study and their clinical data

No.	Sex	Age	Diagnosis	Region	Dose	Dosing period	Underlying disease
MRONJ							
MR01	M	79	MRONJ	Maxilla	Zoledronic acid hydrate Denosumab	4 years 2 months 3 months	Carcinoma
MR02	F	87	MRONJ	Maxilla	Alendronate sodium hydrate	7–8 years	Osteoporosis
MR03	F	87	MRONJ	Mandible	Ibandronate sodium hydrate	8 years	Fracture, rheumatoid arthritis
MR04	M	67	MRONJ	Maxilla	Zoledronic acid hydrate	1 year 3 months	Multiple myeloma
MR05	F	79	MRONJ	Maxilla	Minodronic acid hydrate	3 years	Osteoporosis
MR06	M	70	MRONJ	Maxilla	Denosumab	1 year 4 months	Carcinoma
MR07	F	79	MRONJ	Maxilla	Denosumab	2 years	Carcinoma
MR08	F	81	MRONJ	Mandible	Alendronate sodium hydrate Ibandronate sodium hydrate Denosumab	20 years	Osteoporosis
MR09	F	69	MRONJ	Mandible	Zoledronic acid hydrate Denosumab	4 years 1 year	Carcinoma
MR10	F	62	MRONJ	Maxilla	Zoledronic acid hydrate	9 years	Carcinoma
MR11	F	89	MRONJ	Mandible	Alendronate sodium hydrate Ibandronate sodium hydrate Denosumab	6 years 2 years 6 months	Osteoporosis
MR12	M	82	MRONJ	Maxilla	Alendronate sodium hydrate	5 years	Osteoporosis
MR13	F	84	MRONJ	Maxilla	Minodronic acid hydrate	5 years	Osteoporosis
Osteomyelitis							
OM01	F	96	Osteomyelitis	Maxilla			
OM02	M	47	Osteomyelitis	Mandible			
OM03	F	80	Osteomyelitis	Mandible			
OM04	M	69	Osteomyelitis	Mandible			
OM05	M	65	Osteomyelitis	Mandible			
OM06	M	78	Osteomyelitis	Mandible			
Non-inflammatory bone diseases							
NB01	M	65	Exostosis	Mandible			
NB02	M	43	Jaw deformity	Maxilla and Mandible			
NB03	F	59	Exostosis	Maxilla and palatal			
NB04	M	24	Jaw deformity	Maxilla and Mandible			
NB05	M	70	Exostosis	Maxilla			
NB06	M	55	Jaw deformity	Maxilla and Mandible			
NB07	F	45	Exostosis	Mandible			
NB08	F	27	Jaw deformity	Maxilla and Mandible			
NB09	F	69	Exostosis	Maxilla and palatal			
NB10	M	40	Jaw deformity	Maxilla and Mandible			

10-μm sample was placed on Kapton film (12.5-μm thick; Du Pont-Toray Co., Ltd., Tokyo, Japan) and subjected to elemental distribution analyses. The adjacent section was sliced to a thickness of 4 μm, stained with hematoxylin and eosin (H–E), and subjected to histopathological examination.

Quantitation of the trace-element concentrations in the bone specimens

The specimens of the MRONJ sequestra, osteomyelitis bone, and non-inflammatory bone were weighed while wet and dissolved with concentrated nitric acid (HNO_3; 38 w/v%, UltraPur100, Kanto Chemical Co. Ltd., Tokyo, Japan) overnight at 90 °C. The trace-element concentrations in the solutions were quantitated using ICP-AES (Spectro Arcos, Hitachi High-technologies, Tokyo, Japan). As the standard solutions for ICP-AES analyses, multi-element standard solution (100 ppm, XSTC-22, Seishin Trading Co., Ltd., Kobe, Japan) and Sr standard solution (1000 ppm, Nakarai-tesque, Kyoto, Japan) were used.

Elemental distribution analysis using the synchrotron radiation X-ray fluorescence spectroscopy (SR-XRF) analysis

SR-XRF analyses of the bone specimens were carried out at BL-4A of the Photon Factory at the High Energy Accelerator Research Organization (Tsukuba, Japan). The incident X-ray (12.9 keV) was focused to a region of approximately 30 μm using polycapillary optics, and the specimen was irradiated. The specimen stage was scanned in the X–Y plane to obtain elemental distribution images. The scanning areas varied within several millimeters: the scanning steps varied from 40 μm to 100 μm. The obtained XRF data were processed with PyMCA software (Version 4.7.3) after elemental distribution images were obtained.

Statistical analysis

The statistical analyses of the trace-element contents were performed using JMP software (version 11.2.0, SAS Institute Japan Inc., Tokyo, Japan). The Steel–Dwass test was used to compare trace-element contents among the MRONJ, osteomyelitis, and non-inflammatory bone. The Wilcoxon rank sum test was used to compare trace-element contents before and after decalcification of MRONJ specimens.

Results

Table 2 shows the trace-element contents in the MRONJ sequestra, osteomyelitis bones, and non-inflammatory bones measured by ICP-AES (the contents of Cu and Zn in all specimens are shown in Supplementary Table S1). The content of various trace metallic elements (Co, Cr, Cu, Fe, K, Mg, Ni, Sb, Ti, V, Pb) in MRONJ sequestra was significantly higher than in non-inflammatory bones. Al, Fe K, and Mo content in the osteomyelitis bones was significantly higher than in the non-inflammatory bones. MRONJ sequestra showed significantly higher Cu content (24.3 ppm) compared to both osteomyelitis and non-inflammatory bones. Table 3 shows the comparison of trace-element contents of the MRONJ sequestra between non-treated and decalcified samples. The element content after decalcification was calculated from the wet weight of the specimen before the decalcification treatment. The concentrations of Li, Mo, B, Ba, Fe, Cr, and Cu, were not significantly decreased by the fixation and decalcification. The concentrations of Li and Mo were low both before and after decalcification. The average content of B and Ba did decrease with decalcification, but the difference was non-significant. Concerning Fe and Cr, decalcification caused

Table 2 Element content (ppm) in the specimens measured by ICP-AES

Element	Type of specimens			Statistical analysis		
	MRONJ (MR)	Osteomyelitis (OM)	Non-inflammatory bone (NB)	MR vs OM	MR vs NB	OM vs NB
Al	58.7 (50.9)	72.1 (45.2)	18.3 (9.43)			*
B	45.0 (33.9)	73.3 (64.7)	20.7 (11.1)			
Ba	6.98 (11.6)	3.85 (1.54)	2.51 (1.73)			
Cd	0.32 (0.31)	0.97 (2.15)	0.88 (1.46)			
Co	0.23 (0.38)	0.47 (0.84)	0.75 (0.55)		*	
Cr	1.05 (0.70)	1.60 (1.21)	2.13 (0.91)		*	
Cu	24.3 (34.8)	1.36 (0.92)	0.73 (0.35)	*	*	
Fe	44.8 (19.8)	35.4 (19.5)	6.33 (3.28)		*	*
K	892 (437)	808 (681)	272 (82.7)		*	*
Li	0.87 (1.97)	2.47 (5.91)	2.23 (3.99)			
Mg	1690 (615)	2170 (359)	2390 (233)		*	
Mn	0.09 (0.33)	0.00 (0.00)	0.02 (0.07)			
Mo	0.53 (0.48)	0.37 (0.16)	0.60 (0.19)			*
Na	5440 (1570)	6350 (795)	5490 (632)			
Ni	0.16 (0.55)	0.04 (0.10)	0.40 (0.36)		*	*
Pb	2.77 (1.76)	3.58 (1.73)	4.69 (1.54)		*	
Sb	3.51 (1.67)	4.89 (2.67)	6.41 (1.86)		*	
Ti	0.29 (0.49)	0.45 (0.50)	0.86 (0.46)		*	
V	0.27 (0.35)	0.95 (2.00)	1.33 (1.30)		*	
Zn	85.6 (49.8)	83.0 (20.4)	74.8 (10.9)			
Sr	37.9 (14.5)	41.3 (9.53)	49.2 (9.82)			

Standard deviation is indicated in parentheses,* $p < 0.05$

Table 3 Element content (ppm) in the non-decalcified and calcified MRONJ specimens (for MR01, MR02, MR03, MR05, MR06, MR10) measured by ICP-AES

Element	Non-decalcified	Decalcified	Statistical analysis
Al	40.5 (29.0)	265 (267)	*
B	20.1 (10.9)	9.29 (8.39)	
Ba	5.65 (3.09)	2.41 (4.49)	
Cd	0.47 (0.40)	n.d.	*
Co	0.45 (0.51)	n.d.	*
Cr	1.24 (0.85)	8.44 (20.6)	
Cu	16.8 (15.4)	22.3 (31.7)	
Fe	45.9 (11.4)	84.1 (153)	
K	667 (267)	10.8 (7.18)	*
Li	1.78 (2.74)	1.02 (2.04)	
Mg	1260 (489)	3.28 (2.48)	*
Mn	n.d.	n.d.	
Mo	0.70 (0.68)	0.49 (0.40)	
Na	4900 (1280)	158 (122)	*
Ni	n.d.	n.d.	
Pb	3.18 (1.90)	n.d.	*
Sb	4.09 (1.77)	n.d.	*
Ti	n.d.	n.d.	
V	0.57 (0.32)	n.d.	*
Zn	67.2 (17.1)	4.15 (5.72)	*
Sr	26.9 (11.6)	n.d.	*

Standard deviation is indicated in parentheses, $*p < 0.05$

a nonsignificant increase in their content; the standard deviations of their concentrations after decalcification were also large, suggesting decalcification-induced contamination. On the other hand, Cu content remained stable across decalcification and consequently showed no significant difference, indicating that the accumulated Cu was not dissolved or removed by the decalcification process.

A typical elemental distribution image (S, Ca, Fe, Zn, and Cu) of an entire specimen of MRONJ obtained using SR-XRF with a step of 100 μm step is shown in Fig. 1a. The distribution of each element was visualized as a pseudo-color image. An H–E-stained image of a similar region from adjacent slices is also shown. The entire shape of the specimen and the similarity of the observation area between the two images can be observed in the S-distribution image in Fig. 1a, b. Ca distributions demonstrated no characteristic localization, suggesting that the demineralization of the specimen was successfully completed. Fe was detected in the ICP-AES analysis but could not be detected clearly via the SR-XRF. In contrast, the Cu and Zn distribution images show characteristic distributions in the MRONJ sequestrum. The white-box region of Fig. 1a was analyzed using SR-XRF with a higher resolution (40-μm steps) (Fig. 1b). When referenced to the H–E image, Cu and Zn localization appeared to be situated along the bone trabecula structure. Cu and Zn localization could be identified in the distribution images of other MRONJ specimens when the concentration was high enough (specimens MR01, MR03, MR09, and MR12; Fig. 2). In the osteomyelitis and non-inflammatory bone specimens, no accumulation of trace metallic elements, including Cu and Zn, was observed in their respective elemental distribution images.

Discussion

The present study applied both methods to the quantitative and distribution analysis of the trace elements in MRONJ sequestra and compared their concentrations and distributions with those found in osteomyelitis and non-inflammatory bones. The trace-element contents in MRONJ, osteomyelitis, and non-inflammatory bone specimens were quantitated by the ICP-AES analysis, as shown in Table 2. The trace-element contents of non-inflammatory bones were almost higher than were found by a previous report [13]. We suspect that this difference may be attributed to our not having treated bone specimens before conducting ICP-AES; the previous report washed and dehydrated the bone specimens prior to testing. Some trace elements that dissolve as ionic species in liquid would be removed via the washing and dehydration treatments.

Relative to non-inflammatory bone, the following trace-element contents were found in significantly higher concentrations in the MRONJ sequestra and osteomyelitis bone, respectively: Co, Cr, Cu, Fe, K, Mg, Ni, Sb, Ti, V, and Pb; and Al, Fe, K, and Mo. It is noteworthy to underscore that in both MRONJ and osteomyelitis specimens, Fe and K concentrations were significantly higher than those in non-inflammatory bone. K is one of the major ionic components of body liquid, while Fe in the human body mainly exists in erythrocytes. As both MRONJ and osteomyelitis exhibited inflammation, blood infiltration, and bone degradation, they contained more liquid components, including blood cells, than did the non-inflammatory bone specimen; the K and Fe provided by the increased liquid and blood cells, respectively, thus, accounts for the significantly different concentrations. However, the characteristic accumulation of K and Fe were not clearly observable via SR-XRF. As the SR-XRF specimens were fixed, decalcified, and dehydrated, the trace elements contained in the liquid component may have been removed by the treatment prior to analysis. This further supports our speculation that K and Fe were derived from the liquid component. Because of the large standard deviation, significant differences in the present study were seldom identified. The Al and B in both MRONJ and osteomyelitis specimens showed a higher average concentration relative

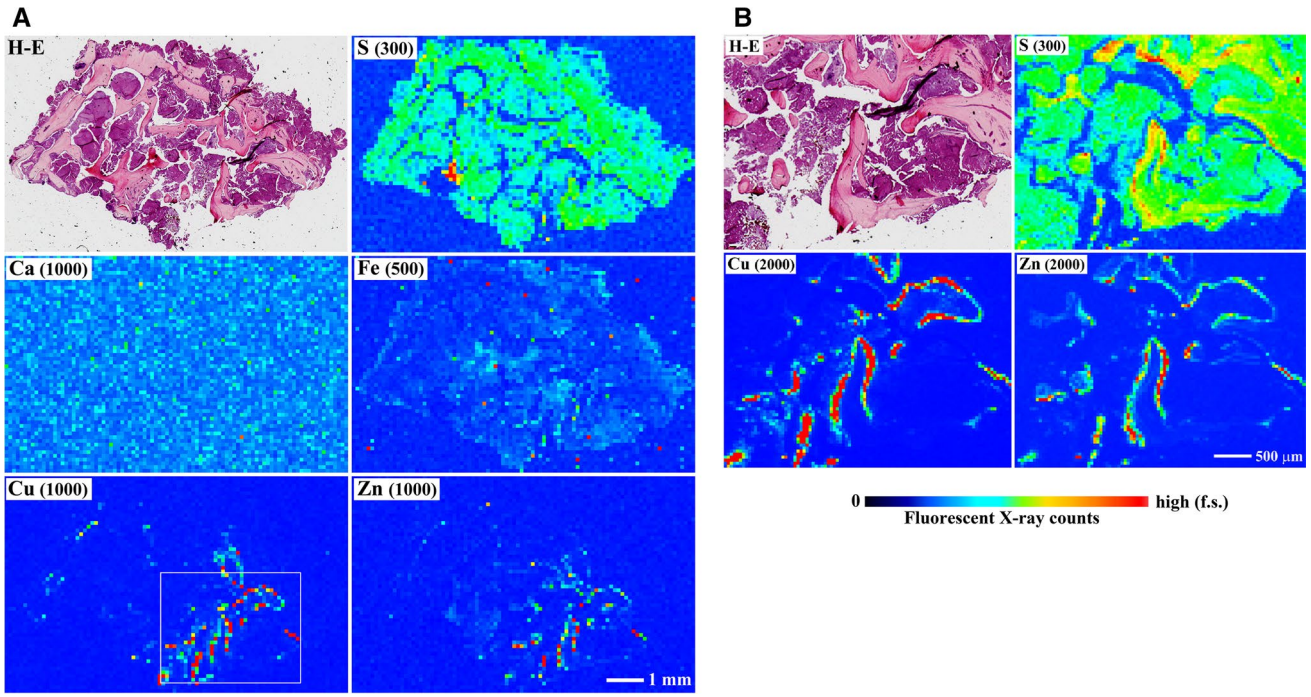

Fig. 1 Histopathological image [hematoxylin and eosin (H–E) staining] and elemental distribution images of MRONJ sequestra specimen (MR07) obtained by SR-XRF. **a** Entire region image (100 μm step), **b** detailed image of the white-box region of Fig. 1a (40 μm step). Numbers in parentheses following the symbol of elements indicate the full scale (f.s.) of fluorescent X-ray counts (count per second) of each element

to those of non-inflammatory bones. The effect of Al and B on bone metabolism has been reported previously [14, 15]; the inflammation or remodeling disorder would cause an abnormal concentration of Al and B. Ni content in MRONJ and osteomyelitis specimens was significantly different from that in non-inflammatory bone diseases (Table 2). However, all Ni contents were in the order of sub-ppm. Therefore, the clinical implications of this difference could not be clearly determined.

In comparison with the trace-element content in osteomyelitis and non-inflammatory bone, the MRONJ sequestra demonstrated a higher concentration of Cu: an average of 24.3 ppm that varied widely, from 3.14 ppm to 132 ppm. As indicated by the elemental distribution analysis with SR-XRF, the variance in Cu accumulation and localization among and within MRONJ sequestra accounts for the large standard deviation of Cu content MRONJ sequestra. However, even at the minimum concentration indicated by the range, Cu content was higher in MRONJ sequestra than in osteomyelitis or non-inflammatory bone. Excess Cu accumulation in MRONJ sequestra was, thus, confirmed.

As shown in Table 3, the concentrations of most of the trace elements decreased after decalcification. The fixation and dehydration processes exchange the liquid component of the specimens, dissolving and removing the ionic species from the specimens. However, the excess Cu remained even after the decalcification process. SR-XRF Cu distribution images show the characteristic distribution of the decalcified specimens (Figs. 1, 2). The Plank–Rychlo solution, which was used for the decalcification process, contains approximately 1 mol/L HCl. The acidic decalcification solution could dissolve the bone apatite, removing the trace elements contained in the apatite thereby. Despite this removal process, Cu contents in MRONJ sequestra were not significantly changed by decalcification. These findings indicate that Cu in MRONJ sequestra was neither dissolved in ionic species, nor was it incorporated in the bone apatite; it likely accumulated in a chemically stable state that could not be dissolved or removed by the acidic decalcification solution.

The SR-XRF Cu distribution image confirms the element's characteristic localization (Figs. 1, 2). The specimens which showed the characteristic distribution of Cu via the SR-XRF also exhibited high concentrations in the ICP-AES test, indicating an agreement between the methods. The H–E-stained image further indicated that the Cu depositions were localized along the trabecular bone (Fig. 1b).

Concerning Zn content, ICP-AES analysis indicated a non-significant difference between the concentrations of the element in the in MRONJ sequestra and non-inflammatory bone. However, SR-XRF analysis revealed a distribution of Zn similar to that exhibited by Cu. As a substituent of Ca, Zn is a minor component of bone apatite but highly

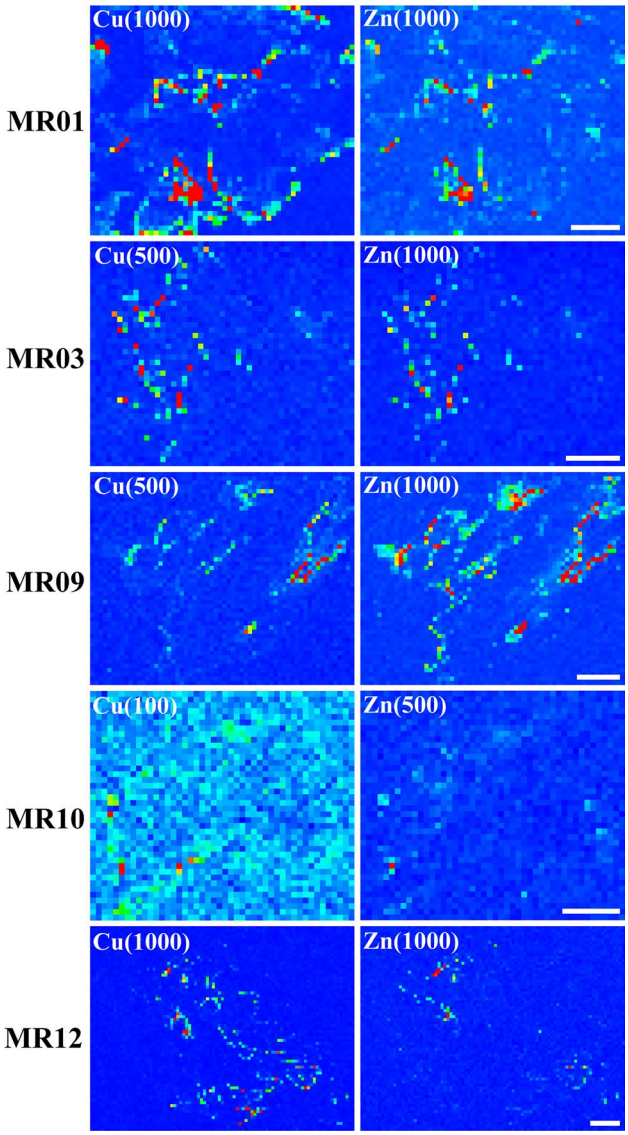

Fig. 2 Cu and Zn distribution images of other MRONJ sequestra specimens obtained by SR-XRF. Numbers in parentheses following the symbol of elements indicate the full scale (f.s.) of the fluorescent X-ray counts (count per second) of each element. White scale bar is equal to 1 mm

concentrated (~100 ppm) relative to Cu (~1 ppm). The variance between the two analyses can be attributed to the decalcification that removed most of the Zn contained in apatite prior to the ICP-AES analysis.

A previous study [12] first visualized characteristic localizations of Cu and Zn in MRONJ sequestra and posited that Cu assumed a chemically stable complex—e.g., BP–Cu complex—in MRONJ sequestra. The characteristic Cu accumulation found by the present study was related to its excessively high concentration; it remained even after decalcification, providing further support for the chemical stability of accumulated Cu in MRONJ sequestra.

Cu is an essential trace metallic element that features an important role in redox reactions and DNA synthesis. Maintaining Cu concentrations within a specific range is essential to health; Wilson' disease and Menkes disease are conditions associated with the overload or deficiency of Cu, respectively [16, 17]. Concerning the relationship of Cu and bone metabolism, the association of Cu deficiency and osteoporosis reportedly contributes to low birth weight among infants [18]. In the case of adults, low serum Cu levels (< 98.5 μg/dL) has been found to correlate with low bone mineral density and high total bone fracture risk [19]. In addition, the potential therapeutic application of supplemental Cu for osteopenia has been reported [20]. On the other hand, the harmful effects of excess Cu have also been reported. Toxic effects were observed for Cu levels higher than 5 μg/mL in chick embryo bone tissue culture media [21], and the presence of Cu levels higher than 2.5 μM caused a decrease in collagen content in the femur due to an inhibition of collagen synthesis [22]. It is also reported that Cu levels higher than 5 μM inhibit in vitro osteogenic differentiation of rat bone marrow mesenchymal stem cells and collagen formation by stem cells implanted in rats [23]. In those in vitro estimations, the Cu content required to express a negative effect was different based on the estimation system, where the thresholds varied and were reported on the order of ppm. In the in vivo estimation, there was a negative correlation between Cu content in bone (0.4–1.1 ng/mg dry wt.) and bone density, Ca content, and collagen content in bone [24]. In another report [19], a group with higher serum Cu levels (> 134 μg/dL) showed the highest fracture risk. Those reports were based on different methods of estimation; therefore, the threshold level of Cu excess could not be determined. However, in those reports, the harmful effect of Cu was exhibited at 5 μg/mL or less. The present investigation estimated the average accumulated Cu content in MRONJ sequestra to be 24.3 ppm (μg/g) (Table 2). As this value represents an average across the entire specimen, the concentrations at the sites of Cu deposits shown in Figs. 1, 2 would be several orders of magnitude above the average value. The Cu concentration in MRONJ sequestra was higher than the threshold noted above from previous studies. Though Cu fulfills essential roles to normative functioning as aforementioned, the excess of Cu found in samples of bone degradation in MRONJ sequestra suggests its potential toxicity.

There were some limitations in this study. First, the derivation of the accumulated Cu could not be determined. The total amount of accumulated Cu in excised sequestra can be calculated from the Cu content and weight. The excised sequestra from the MRONJ patients in this study did not exceed 10 g. Based on the average Cu content (23.9 ppm), the total amount of accumulated Cu in the sequestra per patient would be smaller than 1 mg. The adult human body

contains approximately 50–120 mg of Cu, and the Cu content in serum is in the range of 0.8–1.2 μg/mL [25]. Therefore, the accumulated Cu could originate from the serum. In this study, the serum Cu level could not be determined; this should be estimated in a future study.

Second, the precise structure of accumulated Cu in MRONJ sequestra, as well as the mechanism underlying its suspected toxicity, is also unknown. The inhibition of collagen formation by excess Cu has been reported [22–24], and this might be one of the causes of MRONJ development. Regarding the structure of accumulated Cu, it was assumed to be the BP–Cu complex in a previous report [12]. However, the patients medicated with denosumab in this study, which is a non-BP anti-resorptive agent, also showed Cu accumulation. In those cases, the formation of that complex could not explain the Cu accumulation. In addition, the harmful effect of accumulated Cu was assumed in MRONJ, however, there is still a possibility that Cu accumulation resulted from the disorder of bone metabolism in MRONJ. These possibilities should be investigated in further research.

In conclusion, our study demonstrated significant Cu accumulation and a characteristic distribution of trace metallic elements in MRONJ sequestra. These findings help to elucidate the effect of trace metallic elements on the development of MRONJ. The distribution analysis of the trace metallic elements in bones could serve as a new index to study bone metabolism and related disorders. Moreover, our study demonstrated that the pairing of the quantitative analysis with ICP-AES and distribution analysis with SR-XRF provides complementary information of the trace elements in bone. We believe that this combination could be useful for the analysis of various bone diseases associated with abnormal trace-element content.

Acknowledgements The authors would like to thank Ms. Miwako Hamagaki for the preparation of the specimens for elemental analyses. SR-XRF measurements were performed with the approval of the Photon Factory Program Advisory Committee (Proposal no. 2016G018). This work was supported by a Grant-in Aid from the Japan Society for the Promotion of Science (JSPS no. 16H02688).

Compliance with ethical standards

Conflict of interest The authors declare no conflict of interest.

Ethical approval All patients provided informed consent and the study protocol was approved by the Ethical Committee of Tokyo Medical and Dental University (D2016-002)

References

1. Marx RE (2003) Pamidronate (Aredia) and zoledronate (Zometa) induced avascular necrosis of the jaw: a growing epidemic. J Oral Maxillofac Surg 61:1115–1117
2. Ruggiero SL, Dodson TB, Fantasia J, Goodday R, Aghaloo T, Mehrotra B, O'Ryan F (2014) American Association of Oral and Maxillofacial Surgeons position paper on medication-related osteonecrosis of the jaw—2014 update. J Oral Maxillofac Surg 72:1938–1956
3. Coleman R, Woodward E, Brown J, Cameron D, Bell R, Dodwell D, Keane M, Gil M, Davies C, Burkinshaw R, Houston SJ, Grieve RJ, Barrett-Lee PJ, Thorpe H (2011) Safety of zoledronic acid and incidence of osteonecrosis of the jaw (ONJ) during adjuvant therapy in a randomised phase III trial (AZURE: BIG 01–04) for women with stage II/III breast cancer. Breast Cancer Res Treat 127:429–438
4. Vahtsevanos K, Kyrgidis A, Verrou E, Katodritou E, Triaridis S, Andreadis CG, Boukovinas I, Koloutsos GE, Teleioudis Z, Kitikidou K, Paraskevopoulos P, Zervas K, Antoniades K (2009) Longitudinal cohort study of risk factors in cancer patients of bisphosphonate-related osteonecrosis of the jaw. J Clin Oncol 27:5356–5362
5. Lo JC, O'Ryan FS, Gordon NP, Yang J, Hui RL, Martin D, Hutchinson M, Lathon PV, Sanchez G, Silver P, Chandra M, McCloskey CA, Staffa JA, Willy M, Selby JV, Go AS (2010) Prevalence of osteonecrosis of the jaw in patients with oral bisphosphonate exposure. J Oral Maxillofac Surg 68:243–253
6. Qi WX, Tang LN, He AN, Yao Y, Shen Z (2014) Risk of osteonecrosis of the jaw in cancer patients receiving denosumab: a meta-analysis of seven randomized controlled trials. Int J Clin Oncol 16:403–410
7. Gaudin E, Seidel L, Bacevic M, Rompen E, Lambert F (2015) Occurrence and risk indicators of medication-related osteonecrosis of the jaw after dental extraction: a systematic review and meta-analysis. J Clin Periodontol 42:922–932
8. Kim JW, Kong KA, Kim SJ, Choi SK, Cha IH, Kim MR (2013) Prospective biomarker evaluation in patients with osteonecrosis of the jaw who received bisphosphonates. Bone 57:201–205
9. Marx RE, Cillo JE, Ulloa JJ (2007) Oral bisphosphonate-induced osteonecrosis: risk factors, prediction of risk using serum CTX testing, prevention, and treatment. J Oral Maxillofac Surg 65:2397–2410
10. Lowe NM, Fraser WD, Jackson MJ (2002) Is there a potential therapeutic value of copper and zinc for osteoporosis? Proc Nutr Soc 61:181–185
11. Koçer G, Nazıroğlu M, Çelik Ö, Önal L, Özçelik D, Koçer M, Sönmez TT (2013) Basic fibroblast growth factor attenuates bisphosphonate-induced oxidative injury but decreases zinc and copper levels in oral epithelium of rat. Biol Trace Elem Res 153:251–256
12. Sugiyama T, Uo M, Mizoguchi T, Wada T, Omagari D, Komiyama K, Mori Y (2015) Copper accumulation in the sequestrum of medication-related osteonecrosis of the jaw. Bone Rep 3:40–47
13. Baslé MF, Mauras Y, Audran M, Clochon P, Rebel A, Allain P (1990) Concentration of bone elements in osteoporosis. J Bone Miner Res 5:41–47
14. Chappard D, Bizot P, Mabilleau G, Hubert L (2016) Aluminum and bone: review of new clinical circumstances associated with Al^{3+} deposition in the calcified matrix of bone. Morphologie 100:95–105
15. Newnham RR (1994) Essentiality of boron for healthy bones and joints. Environ Health Perspect 102:83–85
16. Tisato F, Marzano C, Porchia M, Pellei M, Santini C (2010) Copper in diseases and treatments, and copper-based anticancer strategies. Med Res Rev 30:708–749
17. Harvey LJ, McArdle HJ (2008) Biomarkers of copper status: a brief update. Br J Nutr 99:S10–S13
18. Marquardt ML, Done SL, Sandrock M, Berdon WE, Feldman KW (2012) Copper deficiency presenting as metabolic bone

disease in extremely low birth weight, short-gut infants. Pediatrics 130:e1–e4
19. Qu X, He Z, Qiao H, Zhai Z, Mao Z, Yu Z, Dai K (2018) Serum copper levels are associated with bone mineral density and total fracture. J Orthop Transl 14:34–44
20. Rico H, Roca-Botran C, Hernández ER, Seco C, Paez E, Valencia MJ, Villa LF (2000) The effect of supplemental copper on osteopenia induced by ovariectomy in rats. Menopause 7:413–416
21. Rest JR (1976) The histological effects of copper and zinc on chick embryo skeletal tissues in organ culture. Br J Nutr 36:243–256
22. Kaji T, Kawatani R, Takata M, Hoshino T, Miyahara T, Kozuka H, Koizumi F (1988) The effect of cadmium, copper or zinc on formation of embryonic chick bone in tissue culture. Toxicology 50:303–316
23. Li S, Wang M, Chen X, Li SF, Ling L, Xie HQ (2014) Inhibition of osteogenic differentiation of mesenchymal stem cells by copper supplementation. Cell Prolif 47:81–90
24. Massie HR, Aiello VR, Shumway ME, Armstrong T (1990) Calcium, iron, copper, boron, collagen, and density changes in bone with aging in C57BL/6 J male mice. Exp Gerontol 25:469–481
25. World Health Organization (1996) Trace elements in human nutrition and health. World Health Organization, Geneva, pp 123–143. http://www.who.int/nutrition/publications/micronutrients/9241561734/en/. Accessed 15 Oct 2018